strumentation Facility (Grant No. CHE-7818572).

Registry No. Allyl bromide, 106-95-6; cyclopropyl bromide, 4333-56-6; 2-propenyl bromide, 557-93-7; 1-propenyl bromide, 590-14-7; benzene, 71-43-2; anisole, 100-66-3; phenol, 108-95-2; benzene-d_6, 1076-43-3; β-methylstyrene, 637-50-3; cyclopropylbenzene, 873-49-4; allylbenzene, 300-57-2; α-methylstyrene, 98-83-9; *o*-methylstyrene, 611-15-4; *m*-methylstyrene, 100-80-1; *p*-methylstyrene, 622-97-9; indan, 496-11-7; allyl phenyl ether, 1746-13-0; *o*-allylphenol, 1745-81-9; allyl chloride, 107-005-1.

Energetics and Structures of Organosulfur Ions: $CH_3SSCH_3^+$, CH_3SS^+, $C_2H_5S^+$, and CH_2SH^+

James J. Butler,† Tomas Baer,* and Slayton A. Evans, Jr.

Contribution from the Department of Chemistry, University of North Carolina, Chapel Hill, North Carolina 27514. *Received November 30, 1982*

Abstract: The photoionization of dimethyl disulfide (CH_3SSCH_3) yields seven fragment ions between 10.0 and 10.7 eV. Among these are CH_3SS^+ and $C_2H_5S^+$ whose respective measured heats of formation, $\Delta H_f°_{298}$, of 891 and 803 kJ/mol are significantly lower than previously reported. The rate of parent ion dissociation between 10.6 and 10.9 eV forming $C_2H_5S^+$ and H_2CS^+ was measured by photoelectron photoion coincidence. Comparison of the experimental rates with statistically expected rates leads to the conclusion that the dimethyl disulfide ion, which is initially produced with a CSSC dihedral angle of 90°, rearranges to the more stable 180° dihedral angle geometry prior to dissociation. The statistical theory rates fit the measured rates when a 298 K heat of formation of 690 kJ/mol is assumed for the energy of the dimethyl disulfide ion in its lowest energy state. This is 87 kJ/mol lower than previously assumed on the basis of the adiabatic ionization energy. The dimethyl disulfide ion is, therefore, 154 kJ/mol more stable with a CSSC dihedral angle of 180° than with an angle of 90°.

I. Introduction

One of the most striking differences between neutral molecules and the corresponding ions is the geometry of the most stable structure. Classic examples are found in the studies of keto–enol tautomers.[1-3] As a neutral molecule, for instance, the keto form of 2-propanone (acetone) is more stable than its enol tautomer, $CH_2{=}COHCH_3$. However, this relative stability reverses in gas-phase ions where the enol of acetone is 58 kJ/mol more stable than its keto counterpart.[2] Another example of a structural change in the most stable isomer is found in methyl cyanide. As a neutral molecule, the most stable structure is CH_3CN. However, in the ionic form, the structure $CH_2{=}CNH^+$ is 268 kJ/mol more stable than the CH_3CN^+ isomer.[4] Further differences between the most stable structures of neutrals and ions are the radical CH_3O and the ion CH_2OH^+,[5] and HCN and CNH^+.[6] Many of these ionic structures have been verified by ab initio and semiempirical calculations. A very common type of structural transformation is a simple bond-angle change encountered in the ionization of NO_2 to NO_2^+, and NH_3 to NH_3^+, in which the neutral molecule is bent or nonplanar and the ion is linear or planar. Dimethyl disulfide (CH_3SSCH_3) belongs to the latter category in that it has a CSSC dihedral bond angle of 90°, as determined by microwave spectroscopy,[7] while the lowest energy ion, $CH_3SSCH_3^+$, has a dihedral angle of 180° as deduced from both Walsh's rule and CNDO/2 calculations.[8-10] This bond-angle change is evident in the first band of the He I photoelectron spectrum (PES) which is broad, structureless, and rises very slowly.[11] Although an adiabatic ionization energy (IE) of 8.3 eV has been reported, it most likely does not correspond to the 0–0 transition.

Experimental and theoretical studies on the energetics of both diaryl and dialkyl disulfide ions (e.g., $RSSR^+$) are of immense importance because results from these studies should provide a sound basis for understanding the complexities of sulfur–sulfur bonding interactions.[12a] Disulfide bonds also play important roles in maintaining protein structure[12b,c] as well as possessing strong bonding interactions in coal and petroleum extracts.[12d] It is evident that, because of the ease with which disulfides are oxidized to cations, an understanding of the energetics surrounding simple disulfide ions (e.g., $CH_3SSCH_3^+$) will lead to an improved recognition of those factors influencing and ultimately controlling conformational mobility and reactivity of macromolecules containing disulfide bonds.

Numerous mass spectrometric[13-16] and photoelectron[17-19] investigations have been reported on dimethyl disulfide; however, no mass-analyzed photoionization study has been performed. We have undertaken this photoionization study of dimethyl disulfide as part of a continuing program to determine accurate gas-phase heats of formation and structures of organosulfur ions and neutral molecules. This is the first in a series of studies on the structure and energetics of the disulfide linkage in ions.

† Present address: National Bureau of Standards, Washington, DC 21228.

(1) (a) Holmes, J. L.; Terlow, J. K.; Lossing, F. P. *J. Phys. Chem.* **1976**, *80*, 2860. (b) Holmes, J. L.; Lossing, F. P. *J. Am. Chem. Soc.* **1980**, *102*, 3732.
(2) (a) Holmes, J. L.; Lossing, F. P. *J. Am. Chem. Soc.* **1980**, *102*, 1591. (b) Lifshitz, C.; Tzidony, E. *Int. J. Mass Spectrom. Ino Phys.* **1981**, *39*, 181.
(3) Splitter, J. S.; Calvin, M. *J. Am. Chem. Soc.* **1979**, *101*, 7329.
(4) Willett, G. D.; Baer, T. *J. Am. Chem. Soc.* **1980**, *102*, 6774.
(5) Berkowitz, J. *J. Chem. Phys.* **1978**, *69*, 3044.
(6) Bieri, G.; Jonsson, B. O. *Chem. Phys. Lett.* **1978**, *56*, 446.
(7) Sutter, D.; Dreizler, H.; Rudolph, H. D. *Z. Naturforsch. A* **1965**, *20*, 1676.
(8) Kimura, K.; Osafune, K. *Bull. Chem. Soc. Jpn.* **1975**, *48*, 2421.
(9) Van Wart, H. E.; Shipman, L. L.; Scheraga, H. A. *Acc. Chem. Res.* **1974**, *78*, 1848.
(10) Gillbro, T. *Phosphorus Sulfur* **1978**, *4*, 133.
(11) Kimura, K.; Katsumata, S.; Achiba, Y.; Yamazaki, Y.; Iwata, S. "Handbook of HeI Photoelectron Spectra of Fundamental Organic Molecules"; Japan Scientific Society Press: Tokyo, 1980.
(12) (a) Bass, S. W.; Evans, Jr., S. A. *J. Org. Chem.* **1980**, *45*, 710. (b) Boyd, D. B. *J. Am. Chem. Soc.* **1972**, *94*, 8799. (c) Boyd, D. B. *Theor. Chim. Acta* **1973**, *30*, 137. (d) Ahar, A. "Analytical Methods for Coal and Coal Products"; Karr, C., Jr., Ed.; Academic Press: New York, 1979; Vol. 3, Chapter 56, pp 585–624.
(13) Bowie, J. H.; Lawesson, S. O.; Madsen, J. O.; Nolde, C.; Schroll, G.; Williams, D. H. *J. Chem. Soc. B* **1966**, 946.
(14) Cullen, W. R.; Frost, D. C.; Pun, M. T. *Inorg. Chem.* **1970**, *9*, 1976.
(15) Mockel, H. J. *Fresenius Z. Anal. Chem.* **1979**, *295*, 241.
(16) Watanabe, K.; Nakayama, T.; Mottl, J. *J. Quant. Spectrosc. Radiat. Transfer* **1962**, *2*, 369.
(17) Cullen, W. R.; Frost, D. C.; Vroom, D. A. *Inorg. Chem.* **1969**, *8*, 1803.
(18) Coulton, R. J.; Rabalais, J. W. *J. Electron Spectrosc.* **1974**, *3*, 345.
(19) Wagner, G.; Bock, H. *Chem. Ber.* **1974**, *107*, 68.

0002-7863/83/1505-3451$01.50/0

Table I. Appearance Energies (AE in eV) and Heats of Formation (ΔH_f° in kJ/mol) of Major Ions Formed from Dimethyl Disulfide

ion	neutral	AE_{298}	$\Delta H_f^\circ{}_0$	$\Delta H_f^\circ{}_{298}$	$\Delta H_f^\circ{}_{298}$(lit.)
$CH_3SSCH_3^+$		8.33 ± 0.02	707 ± 15[a]	690 ± 15[b]	789.5[c]
CH_3SS^+	CH_3	10.15 ± 0.10	839 ± 8	835 ± 8[b]	971[d]
$C_2H_5S^+$	SH	10.08 ± 0.08	836 ± 8[a]	823 ± 8[e]	828[f]
$CH_3SH_2^+$	HCS	10.5 ± 0.1	711 ± 8	699 ± 8[e]	690[g]
CH_3SH^+	CH_2S	10.4 ± 0.1	904 ± 8	895 ± 8[h]	890[i]
CH_3S^+	CH_3S	10.4 ± 0.1	870 ± 8	862 ± 8[e]	858,[j] 870[k]
CH_2CS^+	CH_3SH	10.15 ± 0.08	979 ± 8[l]	975 ± 8[l]	975[m]

[a] Determined using the RRKM/QET calculation. [b] Calculated using vibrational frequencies from ref 23. [c] Calculated from adiabatic IE of 8.30 eV from ref 18. [d] Reference 14. [e] Calculated using vibrational frequencies constructed from stable molecule in ref 24. [f] Reference 25. [g] Reference 26. [h] Calculated using vibrational frequencies from ref 24. [i] Reference 27. [j] Reference 18. [k] Reference 29. [l] This value was assumed for purposes of the RRKM/QET calculation. [m] Reference 30.

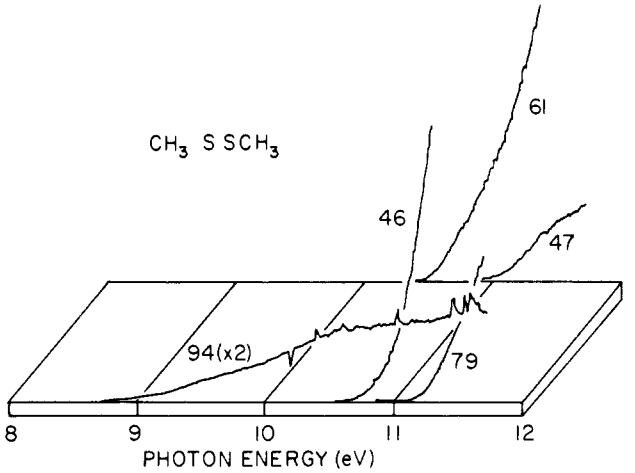

Figure 1. Photoionization efficiency curves for $CH_3SSCH_3^+$ (m/z 94), CH_3SS^+ (m/z 79), $C_2H_5S^+$ (m/z 61), CH_3S^+ (m/z 47), and CH_2S^+ (m/z 46).

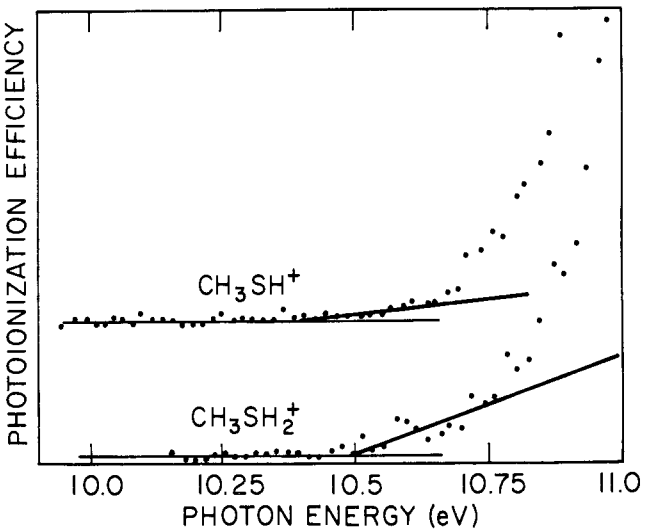

Figure 2. Photoionization efficiency curves of CH_3SH^+ and $CH_3SH_2^+$ from dimethyl disulfide near the dissociation threshold. Ion signals are corrected for ^{34}S contributions.

II. Experiments and Results

The photoionization apparatus has been described previously.[20] Briefly, vacuum UV light from a hydrogen many-line light source dispersed by a 1-m normal incidence monochromator is used to ionize a gaseous sample of dimethyl disulfide. The ions produced are analyzed using a quadrupole mass filter. Photoionization efficiency curves for the various fragment ions are obtained by measuring the signal of mass selected ions as a function of the photon energy. The onsets, or appearance energies (AE), for the various fragmentation paths can then be related to the thermochemistry of the neutral precursor molecule and the ionic and neutral fragments.

The dissociation rates of energy selected dimethyl disulfide ions were studied by threshold photoelectron photoion coincidence (PEPICO). The PEPICO experiment and the technique of extracting the unimolecular dissociation rate of metastable ions from the asymmetrically broadened fragment ion time-of-flight (TOF) distribution have also been described previously.[20,21] At a given photon energy, detection of ions in delayed coincidence with energy-analyzed electrons selects ions of a specific internal energy. In addition, the electron provides the start signal for measuring the ion time-of-flight. The ions are accelerated in an electric field of about 12 V/cm over a distance of 5 cm, pass through a 10-cm drift distance, and are detected by a Spiroltron electron multiplier. Stable parent ions, or fragment ions formed at a fast rate, give rise to narrow and symmetric TOF peaks. However, slowly dissociating ions (metastable ions) fragment at various positions in the acceleration region and therefore result in asymmetric TOF distributions. The parent ion lifetime, or dissociation rate, is determined from the analysis of the asymmetric TOF distribution.

A. Photoionization Efficiency Curves. The photoionization efficiency (PIE) curves for the parent ion and four fragment ions are shown in Figure 1. These curves are corrected for the quadrupole mass filter collection efficiency and are normalized with respect to each other. The nonnormalized PIE curves for CH_3SH^+ (m/z 48) and $CH_3SH_2^+$ (m/z 49) ions are presented separately in Figure 2. These curves were corrected for the contribution of $CH_2{}^{34}S^+$ to the m/z 48 signal and $CH_3{}^{34}S^+$ to the m/z 49 signal. Appearance energies (AE) at 298 K for each ion were obtained by linear extrapolation of the PIE curves to the base line near their onsets. These onsets were converted to 0 K onsets by adding to the 298 K onset the thermal internal energy of the neutral dimethyl disulfide molecule as described by Fraser-Monteiro et al.[22] The $\Delta H_f^\circ{}_0$ is then calculated using the relation:

$$\Delta H_f^\circ{}_0(AB) + AE(0\ K) = \Delta H_f^\circ{}_0(A^+) + \Delta H_f^\circ{}_0(B)$$

where AB, A^+, and B are the molecular precursor, the fragment

Table II. Auxiliary Heats of Formation of Neutral Molecules and Fragments (kJ/mol)

molecule	$\Delta H_f^\circ{}_{298}$	$\Delta H_f^\circ{}_0$
CH_3SSCH_3	−24.2[a]	−6.8[b]
CH_3SH	−22.3[a]	−12.1[a]
CH_3S	136.0[c]	143.0[d]
CH_2S	102.0[e]	105.0[d]
HCS	305.0[f]	310.0[g]
SH	143.0[h]	142.0[h]
CH_3	142.3[h]	145.6[h]

[a] Reference 31. [b] Calculated using vibrational frequencies from ref 23. [c] Reference 32. [d] Calculated using vibrational frequencies from ref 24. [e] Reference 33. [f] Reference 20. [g] Calculated using vibrational frequencies from ref 34. [h] Reference 27.

(20) Butler, J. J.; Baer, T. *J. Am. Chem. Soc.* **1980**, *102*, 6764.
(21) Baer, T. In "Gas Phase Ion Chemistry"; Bowers, M. T., Ed.; Academic Press: New York, 1979; Chapter 5.
(22) Fraser-Monteiro, M. L.; Fraser-Monteiro, L.; Butler, J. J.; Baer, T.; Hass, J. R. *J. Phys. Chem.* **1982**, *86*, 739.

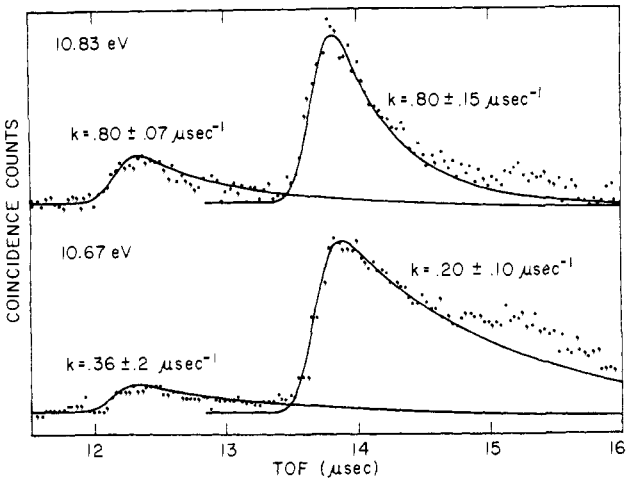

Figure 3. Fragment ion time-of-flight (TOF) distributions for CH_2S^+ at 12.2 μs and $C_2H_5S^+$ at 13.6 μs. Solid lines are calculated TOF distributions assuming the indicated dissocation rates.

ion, and product neutral, respectively. Appearance energies and the derived heats of formation of the observed ions are presented in Table I, while Table II lists the auxiliary heats of formation used in the construction of Table I.

B. Dissociation Rates of Metastable $CH_3SSCH_3^+$. In the energy region near the onsets of the CH_3SS^+ (m/z 79), $C_2H_5S^+$ (m/z 61), and CH_2S^+ (m/z 46) fragment ions, $CH_3SSCH_3^+$ is metastable. Evidence for the slow dissociation of parent ions is seen in the asymmetric TOF peaks for CH_2S^+ and $C_2H_5S^+$ of Figure 3. In order to minimize instrumental broadening of the TOF peaks, no quadrupole mass filter was used in these rate studies. Under these conditions the CH_3SS^+ ion appears as a small shoulder on the tail of the much larger $C_2H_5S^+$ ion peak. Because of its small contribution, no dissociation rates to the CH_3SS^+ ion could be measured. In addition, metastable time-of-flight distributions could only be obtained at energies between 10.6 and 10.9 eV. The m/z 46 signal was extremely small below 10.6 eV so that no meaningful data could be obtained below this energy. Above 10.9 eV, the m/z 47, 48, and 49 signals were greater than 5% of the total ion signal and interferred with the analysis of the m/z 46 ion signal.

Within the experimental error, the measured decay rates to m/z 46 and 61 are identical and equal to the total dissociation rate. This indicates that the two fragmentation paths have the same $CH_3SSCH_3^+$ precursor ion, which dissociates competitively via the two paths. This fact allows us to determine the individual rates of fragmentation to the two products by combining the total rates with the relative rates obtained from the areas under the peaks in Figure 3. These derived rates are shown in Figure 4.

III. Discussion

A. Thermochemistry. In order to interpret the rate data, it is essential to analyze the thermochemistry in detail. Product ion

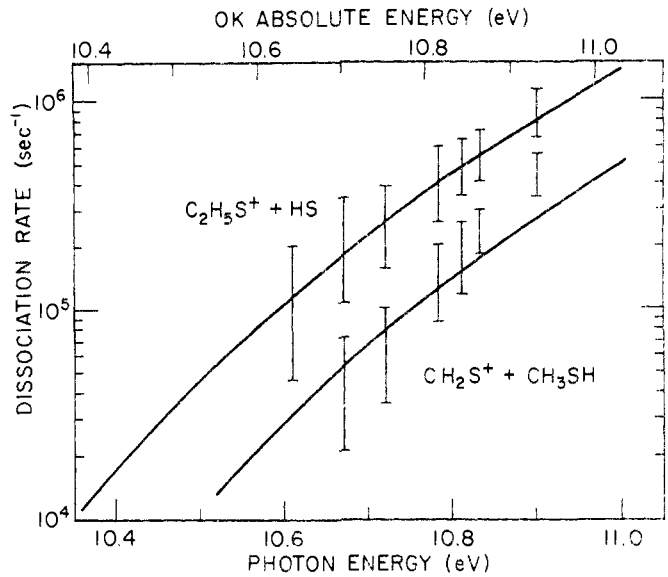

Figure 4. The decay rate as a function of ion energy for the dissociation of dimethyl disulfide. The 0 K absolute energy scale is based on the dimethyl sulfide molecule in the ground vibration and rotation state. The photon energy scale includes the molecular thermal energy.

heats of formation calculated from appearance energies which are obtained from PIE curves are often upper limits to the true thermochemical heats of formation as a result of reverse activation barriers and kinetic shifts. The latter arise because of slow dissociation rates which shift observed onsets to higher energies. In the case of metastable dissociations, as we have here for m/z 46 and 61, it is possible to use the statistical theory fit to the rate data and extrapolate the rates to the true onsets, thereby overcoming the problem of the kinetic shift.

1. $CH_3SSCH_3^+$ (m/z 94). The IE of 8.33 eV measured from the parent ion PIE curve is in good agreement with the reported adiabatic PES value of 8.3 eV.[11,18] However, as was already pointed out and is also evident from the dissociation rates (vide infra), this value is not the true adiabatic IE. On the basis of the comparison between measured and calculated dissociation rates we determined the adiabatic IE to be 7.4 ± 0.3 eV, yielding a 298 K heat of formation of 690 kJ/mol.

2. CH_3SS^+ (m/z 79). This ion has a very weak onset at 10.15 eV and clearly appears as a shoulder on the asymmetric m/z 61 peak (Figure 3). A much stronger onset is evident at 11.10 eV. It seems probable that this ion is formed by a direct S–CH_3 bond cleavage above 11.10 eV, and that its structure at this energy is CH_3–S–S^+. Between 10.15 and 11 eV, a more stable isomer may be formed via a "tight" transition state.

3. $C_2H_5S^+$ (m/z 61). This is the ion formed via the lowest energy dissociation pathway. From the statistical theory fits to the rate data, we calculate a 0 K onset of 10.00 eV which corresponds to a 298 K onset of 9.88 eV. The observed onset of 10.08 eV is evidently shifted by 0.2 eV as a result of the slow dissociation rate. We can check the reasonableness of this hypothesis. In the PIE experiment the ions need approximately 10 μs to reach the quadrupole mass filter. Suppose that our sensitivity for observing a fragment ion is 1%. If only 1% of the slowly dissociating parent ions form products prior to entering the mass filter, a signal would be detected. This corresponds to a rate, k, given by $1 - \exp(k \times 10\ \mu s) = 0.01$, of $10^3\ s^{-1}$. The RRKM/QET calculation of Figure 4 reaches a rate of 10^3 at 0.28 eV above the dissociation onset which is very close to the derived kinetic shift of 0.2 eV. Thus, the PIE onset and the rate data are in excellent agreement. We derive a $\Delta H_f°_{298}(C_2H_5S^+)$ of 803 ± 8 kJ/mol. Previous electron impact determinations of the heat of formation have yielded values of around 828 kJ/mol.[25] However, these onsets, from which the heat of formation was derived, were also affected by the kinetic shift as well as the usual problems associated with nonenergy selected electron impact so that the present value is more reliable. The structure derived on the basis of both collisional

(23) Frankiss, S. G. *J. Mol. Struct.* **1969**, *3*, 89.
(24) Shimanouchi, T. *Natl. Stand. Ref. Data Ser., Natl. Bur. Stand.* **1972**, No. 39.
(25) Broer, W. J.; Weringa, W. D.; Nieuwpoort, W. C. *Org. Mass Spectrom.* **1979**, *14*, 543.
(26) Keyes, B. G.; Harrison, A. G. *J. Am. Chem. Soc.* **1968**, *90*, 5671.
(27) Rosenstock, H. M.; Draxl, K.; Steiner, B. W.; Herron, J. T. *J. Phys. Chem. Ref. Data Suppl.* **1977**, *6*, 1.
(28) Akopyan, M. E.; Sergiev, Y. L.; Vilesov, F. I. *Khim. Vys. Energ.* **1970**, *4*, 265, 306.
(29) Roy, M.; McMahon, T. B. *Org. Mass Spectrom.* **1982**, *17*, 392.
(30) Butler, J. J.; Baer, T. *Org. Mass Spectrom.*, in press.
(31) Pedley, J. B.; Rylance, J. "Sussex-NPL Computer Analyzed Thermochemical Data: Organic and Organo-metallic Compounds" University of Sussex: Sussex, England, 1977.
(32) Benson, S. W. "Thermochemical Kinetics"; Wiley: New York, 1976.
(33) Jones, A.; Lossing, F. P. *J. Phys. Chem.* **1967**, *71*, 4111.
(34) Butler, J. J.; Baer, T. *J. Am. Chem. Soc.* **1982**, *104*, 5016.

Table III. Molecular Ion and Transition-State Frequencies of Dimethyl Disulfide Used in the RRKM/QET Calculations[a]

3000, 3000, 2990, 2990, 2930, 2930, 1430, 1425, 1420, 1415, 1310, 1310, 960, 960, 950, 880, 695, 695, 510,[b] 272, 242, 134, 134, 106

[a] Frequencies from ref 23. [b] Assumed reaction coordinate.

activation[25,35] and ab initio calculations[25] is $CH_2{=}S^+{-}CH_3$.

4. CH_3SH^+ (m/z 49). The PIE of CH_3SH^+, shown in Figure 2, is associated with a higher energy fragmentation path and is, therefore, subject to a kinetic shift because of the competition of this fragmentation with faster, lower energy, dissociation paths. As a result, the onset was chosen as low as the data would permit. This 10.4-eV onset yields in turn a heat of formation of 895 ± 8 kJ/mol which is in excellent agreement with the 890-kJ/mol value derived from the photoionization of CH_3SH;[27] that is, there is no kinetic shift. This is rather remarkable because an onset of 10.4 eV should result in an extremely slow dissociation rate at the fragmentation threshold. Because the formation of $CH_3SH^+ + H_2CS$ involves some rearrangement, it is difficult to argue in favor of a rapid direct dissociation. We suggest that the 10.4 eV onset is fortuitous, and that perhaps a more stable ion is being formed, such as $H_2C{=}SH_2^+$. The onset at 10.4 eV is then simply the energy at which the dissociation rate becomes sufficiently large to be detectable.

5. CH_3S^+ (m/z 47). There appears to be increasing agreement that the structure of this ion is CH_2SH^+.[29,36] Our heat of formation of 862 kJ/mol is considerably lower than an upper limit to this value recently reported by us on the basis of a photoionization study of tetrahydrothiophene. The new, lower value found here is consistent with a photoionization result of Akopyan et al.[28] of 858 kJ/mol, and a recent value of 870 kJ/mol reported by Roy and McMahon.[29]

6. CH_2S^+ (m/z 46). The second fragment formed by the metastable parent ion is CH_2S^+. It, and its neutral partner, CH_3SH, have well-established heats of formation. The value of 975 kJ/mol for $\Delta H_f°_{298}(CH_2S^+)$ is based on a photoionization study of thietane and tetrahydrothiophene in which CH_2S^+ is a low-energy, and dominant, fragmention.[30] Its structure is probably that of the enol, $CHSH^+$. The neutral fragment, CH_3SH, is stable and has a well-known heat of formation. No structure other than methanethiol appears likely. As a result we can establish a 0 K onset of 10.10 eV which corresponds to 10.22 eV at 298 K. Comparing this to the 10.15-eV measured onset indicates that there is a 0.07-eV kinetic shift.

The precise knowledge of this onset is important information for analyzing the rate data of Figure 4. Because the CH_2S^+ PIE curve is displaced from that of $C_2H_5S^+$ by just 0.1 eV, a 0 K onset of 10.00 eV for the latter ion can be established. This, in turn, allows the $CH_3SSCH_3^+$ energy to be determined.

B. Dissociation Rates and $CH_3SSCH_3^+$ Energy. The rate data of Figure 4 were compared with RRKM/QET calculated rates. The input to these calculations are the activation energy and the vibrational frequencies of the precursor ion and transition state. The frequencies of CH_3SSCH_3 (Table III) were used for both the molecular ion and the transition state. The activation energies can be calculated from the differences in the dissociation limits (10.00 and 10.10 eV for the two fragment ions) and the ionization energy of the molecular ion. The latter value obtained from PES is 8.3 eV. Rate calculations on the basis of this 1.7-eV activation energy were found to be 1000 times greater than our measured rates. The rates could be reduced by drastically increasing the vibrational frequencies of the transition state, making it a very "tight" transition state. But this had the effect of reducing the slope of the $k(E)$ vs. E curve.

We considered the possibility that the parent ion isomerizes to a more stable structure prior to dissociation. This has the effect of increasing the activation energy in the dissociation step and would result in lower calculated rates. A number of isomers were considered, among them $HSCH_2CH_2SH^+$ and $CH_3CH_2SSH^+$. However, these could be ruled out because they are known to have higher energies than the dimethyl disulfide ion (see Table IV). To our knowledge, there are no data available for the ion $CH_3SCH_2SH^+$. We assumed its heat of formation to be intermediate between that of $HSCH_2CH_2SH^+$ and $CH_3SSCH_3^+$, and thus also rule it out as a candidate for the lower energy isomerized form. Because the $CH_3SSCH_3^+$ dihedral angle changes from 90 to 180° upon ionization, it is reasonable to suppose that the true adiabatic ionization energy is lower than the measured 8.3 eV. We, therefore, carried out a series of RRKM/QET calculations in which the parent ion energy was varied until a good fit to the experimentally measured rates was found. This gave an adiabatic ionization energy of 7.4 eV, which is 1 eV lower than the measured value.

A diagram of the potential energy as a function of dihedral angle is shown in Figure 5. The photoelectron spectrum of the first band is sketched in this figure to show the Franck–Condon overlap between the CH_3SSCH_3 molecule and ion. We note that there is an approximate energy difference of 1.6 eV between the ion structure with a dihedral angle of 90° and that of the most stable structure at 180°. This energy difference has been determined[10] by a semiempirical CNDO/2 calculation to be 0.9 eV. If we consider that the CNDO/2 program was probably not optimized for such calculations with sulfur atoms, we cannot expect more than qualitative agreement between the experimental and calculated results. Ab initio calculations with extended basis sets such as the 6-31G* are necessary in order to calculate this energy difference quantitatively.

Table IV. Thermochemistry of Three $C_2H_6S_2$ Isomers

molecule	neutral $\Delta H_f°_0$ (kJ/mol)	IE (eV)	ion $\Delta H_f°_0$ (kJ/mol)
CH_3SSCH_3	−6.8[a]	8.3[b]	794[c]
$SHCH_2CH_2SH$	11.3[a]	9.3[d]	908
CH_3CH_2SSH	−9[e]	9.4[f]	898

[a] Calculated using $\Delta H_f°_{298}$ of ref 31 and vibrational frequencies of ref 23. [b] Reference 18. [c] For purposes of this comparison we use the adiabatic IE of 8.3 eV. [d] This work. [e] Calculated using group additivity of Benson (ref 32). [f] Calculated by semiempirical interpolation in ref 37.

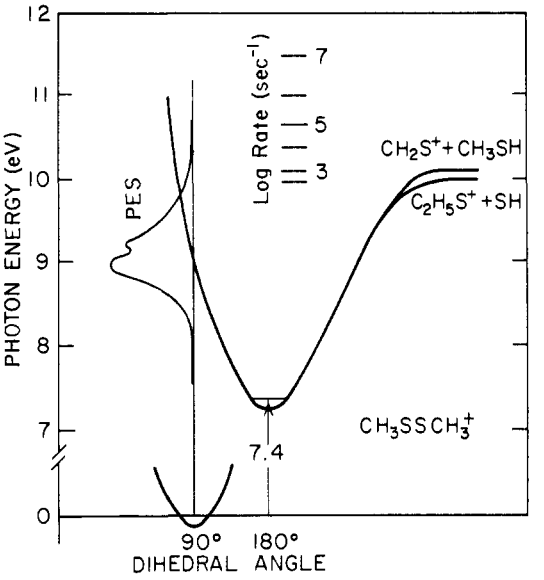

Figure 5. Potential energy diagram showing schematically the energies of the dimethyl disulfide molecule and ion as a function of the dihedral angle. The photoelectron spectrum is taken from ref 11.

(35) van der Graaf, B.; McLafferty, F. W.; *J. Am. Chem. Soc.* **1977**, *99*, 6806.
(36) Dill, J. D.; McLafferty, F. W. *J. Am. Chem. Soc.* **1978**, *100*, 2907.
(37) Levitt, L. S.; Parkanyi, C. *Int. J. Sulfur Chem.* **1973**, *8*, 329.

IV. Conclusion

Accurate heats of formation of $C_2H_5S^+$ and CH_2S^+ ions and the measured dissociation rates of energy-selected dimethyl disulfide ions are used to show that the dimethyl disulfide ion has a dihedral angle of 180° and that its energy is 1.6 eV more stable than the ion with a dihedral angle of 90°. The ionization energy of the dimethyl disulfide is calculated to be 7.4 eV on the basis of RRKM/QET calculations. This is 0.9 eV lower than the adiabatic ionization energy of 8.33 eV measured by PES.

Acknowledgment. We are greatful to the Department of Energy for the support of this work.

Registry No. CH_3SSCH_3, 624-92-0; CH_3SS^+, 12538-77-1; $C_2H_5S^+$, 20828-74-4; $CH_3SSCH_3^+$, 34628-72-3; CH_3SH^+, 53369-41-8; CH_3S^+, 20828-73-3; CH_2S^+, 61356-81-8.

Kinetic Parameters for a System at Equilibrium from the Time Course of Luminescence Emission: A New Probe of Equilibrium Dynamics. Excited-State Europium(III) as a Species Label

William DeW. Horrocks, Jr.,* Valerie K. Arkle, Frank J. Liotta, and Daniel R. Sudnick

Contribution from the Department of Chemistry, The Pennsylvania State University, University Park, Pennsylvania 16802. *Received September 15, 1982*

Abstract: Forward and reverse rate constants for the equilibrium between the europium(III) complex of 1,2-diaminocyclohexanetetraacetate, $Eu(DCTA)^-$, and iminodiacetate, $IMDA^{2-}$, to form the ternary complex $Eu(DCTA)(IMDA)^{3-}$ are obtained from the time course of luminescence emission following selective laser excitation of the Eu(III)-containing species. This new method depends upon selective excitation of the $^7F_0 \rightarrow {}^5D_0$ electronic transition of a particular Eu(III) species while monitoring the time course of luminescence emission, either predominately from the same species or from one into which it is converted chemically, at a rate comparable to the reciprocal lifetime of the excited state of the species involved. Since excited state Eu(III) has the same reactivity in ligand-exchange reactions as the ground-state ion, the electronic excitation acts as a species label in a manner analogous to the use of nuclear spin saturation transfer as a nuclear label. Twelve different luminescence emission curves obtained at three different pH values (four permutations of λ_{ex} and λ_{em} at each pH) were fit with a total of five adjustable parameters. At 23.5 °C the following results were obtained: $k_f = 1.6 \times 10^7\ M^{-1}\ s^{-1}$, $k_r = 2.6 \times 10^3\ s^{-1}$, $K_{eq} = 6.3 \times 10^3\ M^{-1}$, $\tau_{Eu(DCTA)^-} = 0.320$ ms, $\tau_{Eu(DCTA)(IMDA)^{3-}} = 0.805$ ms. Other systems wherein chemical interconversion processes occur at rates much greater than (rapid exchange) or much slower than (slow exchange) the reciprocal excited-state lifetime of the Eu(III)-containing species are briefly examined. Eu(III) complexes of the ligands oxydiacetate and dipicolinate are examples of the former and latter, respectively.

Methods for obtaining kinetic information on systems at equilibrium rely on experiments that sample separate environments of interconverting species on a time scale comparable to that of the chemical rate process of the interconversion. Examples in current use include dynamic NMR methods,[1,2] nuclear spin saturation transfer,[3] EPR line broadening,[4] and fluctuation spectroscopy.[5] In dynamic NMR,[1,2] parameters are determined for processes that occur at rates comparable to the chemical shift difference (expressed in frequency units) between nuclei in interconverting environments. Nuclear spin saturation transfer[3] monitors rates comparable to the spin–lattice relaxation times of a nucleus shuttling between two environments. EPR line-broadening techniques[4] have proven useful particularly in the study of the rates of electron-transfer reactions. The fluctuation spectroscopic technique[5] of determining kinetic parameters is based on the principle that the rates of decay of spontaneous microscopic fluctuations are determined by the same rate constants as those for a macroscopic departure from equilibrium. The essence of most of these methods is the ability of an experiment to track a label, e.g., a chemical shift difference or degree of nuclear saturation, of interconverting chemical species on a time scale comparable to the interconversion rate. We report here a new method for obtaining kinetic information on a system at equilibrium where the label involved is the excited $^5D_0$ emissive state of Eu(III) and the kinetic process is monitored via the time course of luminescence emission.[6]

Experimental Section

The principal chemicals used were obtained from the suppliers indicated: 1,2-diaminocyclohexanetetraacetic acid, H_4DCTA (Aldrich); dipicolinic acid, H_2DPA (Eastman); iminodiacetic acid, H_2IMDA (Sigma); oxydiacetic acid, H_2ODA (Fluka AG); europium(III) chloride hexahydrate (Aldrich). All other chemicals were reagent grade or the purest commercially available.

The time course of luminescence emission was measured by using a pulsed nitrogen laser pumped dye laser apparatus described in detail elsewhere.[7,8] Individual emissions were recorded with the aid of a transient digitizer and signal averager. The data (1900 points per curve) were then computer fit by using every tenth or every fifth point to the theoretical expressions (vide infra) employing an IBM share program designated NLIN2, an algorithm for least-squares estimation of nonlinear parameters.[9]

(1) Sandstrom, J. "Dynamic NMR Spectroscopy"; Academic Press: New York, 1982.
(2) Jackman, L. M.; Cotton, F. A. "Dynamic Nuclear Magnetic Resonance Spectroscopy"; Academic Press: New York, 1975.
(3) Gupta, R. K.; Redfield, A. G. *Science (Washington, D.C.)* **1970**, *169*, 1204–1206.
(4) Li, T. T.-T.; Brubaker, C. H., Jr. *J. Organomet. Chem.* **1981**, *216*, 223–224 and references therein.
(5) Weissman, M. B. *Ann. Rev. Phys. Chem.* **1981**, *32*, 205–232.
(6) Kinetic information has, of course, been obtained from the fluorescence of organic molecules; however, excited-state organic molecules have a chemical reactivity different from their ground-state counterparts, and such systems are not in equilibrium following excitation. See: Weller, A. *Prog. React. Kinet.* **1961**, *1*, 187–214.
(7) Sudnick, D. R. Ph.D. Thesis, The Pennsylvania State University, 1979.
(8) Horrocks, W. DeW., Jr.; Sudnick, D. R. *Acc. Chem. Res.* **1981**, *14*, 384–392.

0002-7863/83/1505-3455$01.50/0